Simulation of Plasma Flow in the Edge Region of a Stellarator

M.A. Hussein, G.A. Emmert

February 1989

UWFDM-790

FUSION TECHNOLOGY INSTITUTE

UNIVERSITY OF WISCONSIN

MADISON WISCONSIN

Simulation of Plasma Flow in the Edge Region of a Stellarator

M.A. Hussein, G.A. Emmert

Fusion Technology Institute
University of Wisconsin
1500 Engineering Drive
Madison, WI 53706

http://fti.neep.wisc.edu

February 1989

UWFDM-790

Simulation of Plasma Flow in the Edge Region of a Stellarator

Makarem A. Hussein and G.A. Emmert
Nuclear Engineering and Engineering Physics Department
University of Wisconsin-Madison, Madison, Wisconsin 53706

Abstract

A kinetic code to simulate collisionless magnetized plasma flow along expanding magnetic field lines to a neutralizer plate is developed and presented. A Monte Carlo description for the ion dynamics coupled with Boltzmann electrons is used to develop an iterative scheme for the Vlasov equation and quasi-neutrality. The electrostatic potential profile, the potential drop in the sheath, and particle and energy fluxes to the wall are calculated. The code has been used to simulate plasma flow in the edge region of stellarators with expanding magnetic field lines and neutral gas recycling at the neutralizer plate.

1 Introduction

The problem of a plasma flowing to a neutralizer plate is very common in fusion devices as well as in plasma processing techniques. Generally, a plasma striking a collector plate is neutralized and the resulting gas molecules evolved from the plate interact with the incoming plasma by atomic processes, such as dissociation, charge exchange, and ionization. This produces cold ions which increase the plasma density near the plate. If the electrons are sufficiently collisional to remain close to a Maxwellian distribution, then the electrostatic potential will also increase following the Boltzmann relation. In the presence of an expanding magnetic field, ions will be accelerated towards the plate and their density will drop accordingly. This competes with the increased ion density in determining the electrostatic potential profile. Knowledge of this potential variation in a collisionless plasma is the key to knowing other plasma parameters, such as the density profile and particle and energy fluxes to the wall.

In this paper, we are concerned with the plasma flow to a neutralizer plate in the divertor chamber of a toroidal magnetic fusion system. A number of kinetic models have been developed to describe this problem. Hinton and Hazeltine [1] considered the structure of the plasma boundary in a tokamak with a poloidal divertor. They assumed hot collisionless ions, and cold collisional electrons and described plasma diffusion across the separatrix and particle motion along the field line by a kinetic equation. The same ba-

sic assumptions were considered by El-Nadi [2] to show the importance of the barely trapped ions in determining the radial profiles. Daybelge [3] developed a 2-D model for the plasma scrape-off layer which shows how the plasma transport is modified by the interaction with the collector plates, leading to induced asymmetries at the plasma edge of a tokamak. He solved the ion-drift kinetic equation for a guiding center distribution function and a Fokker-Planck collision operator for the ion-ion collisions.

Gierszewski *et al.* [4] studied the structure of plasma near a target plate by using a kinetic transport model which includes binary collision processes between the various ion, atomic and molecular species, and the self-consistent electrostatic field. The magnetic field, however, was uniform. Emmert and Bailey [5] considered the plasma flow through a magnetic field with a constriction (as in a bundle divertor). They included the effect of the neutrals refluxing from the target plate and the related atomic processes, *e.g.* ionization and charge exchange [6].

In this work we developed a kinetic code which is capable of simulating the plasma flow to a divertor plate self-consistently with the electrostatic field and in the presence of a monotonically falling external magnetic field. The ion motion is assumed to be collisionless on the scale length of the magnetic field variation. We also include the effect of electron impact ionization of the neutral gas refluxing from the target plate. The mathematical formulation of the problem is given in Section 2. Also discussed in this section is the method used to compute ion trajectories, which are basic ingredients in our

model. The numerical algorithm we use is outlined in Section 3. Section 4 discusses the effects of neutral gas recycling. Modeling considerations related to stellarator divertor structures are given in Section 5. The simulation results are given in Section 6 and our conclusions are presented in Section 7.

2 Mathematical Formulation

The flow of a collisionless plasma along field lines in the edge region is determined by:

1. The Vlasov equation for ions,

$$\mathbf{v} \cdot \nabla f_i + \frac{\mathbf{F}}{m_i}(\frac{\partial f_i}{\partial \mathbf{v}}) = S \ , \tag{1}$$

   where $\mathbf{F}$ is the force on an ion with mass m_i, velocity $\mathbf{v}$, distribution function f_i, and S is the source term for these ions.

2. Quasi-neutrality along field lines,

$$n_e(x) = n_i(x) = \int f_i \, d\mathbf{v} \ , \tag{2}$$

   where n_e and n_i are the electron and ion densities, respectively. This assumes the Debye length is small compared with macroscopic scale lengths.

3. A Boltzmann distribution of electrons with temperature T_e,

$$n_e(x) = n_{eo} \ \exp(\frac{e\Phi(x)}{KT_e}) \ , \tag{3}$$

where $\Phi(x)$ is the electrostatic potential, n_{eo} is the electron density at $x = 0$ where Φ is defined to be zero, e is the electron charge, and K is the Boltzmann constant.

Our approach to solving this system of equations parallels that developed by Whealton *et al.* [7] in which the Vlasov equation is solved indirectly by computing ion trajectories in the self-produced electrostatic potential and the externally applied magnetic field. The ions are assumed to be emitted from sources distributed along the computational mesh with random velocities sampled from a probability distribution [8] of the form

$$f(v) = 2\beta v \exp(-\beta v^2) . \tag{4}$$

This gives a Maxwellian particle distribution in the absence of an electrostatic potential gradient. It follows from Eq. (4) that for a randomly chosen number p_i, selected by sampling on a uniform interval [0,1], the corresponding random velocity v_i is given by

$$v_i = \sqrt{-\frac{2KT_i}{m_i} \ln p_i} \quad , \tag{5}$$

where T_i is the ion source temperature. The direction of travel is determined by another randomly chosen number on the uniform interval [0,1]. Generating velocities with the above method will produce equal statistical weights for all the ions. The collisionless motion of an ion in the electrostatic potential $\Phi(x)$ and the externally applied electric field is described by

$$m_i \frac{dv_{\|}}{dt} = q\left(-\frac{d\Phi}{dx} - \mu\frac{dB(x)}{dx}\right) \tag{6}$$

and

$$\frac{dx}{dt} = v_{\|} \tag{7}$$

where x is the coordinate along a field line, q is the ion charge, $B(x)$ is the vacuum magnetic field strength, $v_{\|}$ is the ion velocity along the field line, and μ is the magnetic moment of an ion.

Once an ion is launched from a given source, its trajectory is calculated using the above equations in the region $0 < x < L$. We divide the computational region, as shown in Figure 1, into cells of width Δx, and assume the acceleration is constant in each cell. The time spent by an ion in the jth cell is then calculated. The ion density in the jth cell is then given by

$$n_j = \sum_{i,k} S_i \frac{\Delta t_{ijk}}{\Delta x_j} \frac{B(x_j)}{B(x_i)} \ , \tag{8}$$

where t_{ijk} is the time spent in the jth cell of width Δx_j by the kth particle launched from the ith source of strength S_i. The term $B(x_j)/B(x_i)$ models the expansion of the magnetic flux tube as the particles follow the magnetic field. A trajectory is terminated whenever it hits the plate at $x = L$. With no neutral gas recycled, the plate at $x = L$ is assumed to be electrostatically floating and perfectly absorbing. This means that no ions are to be reflected from the plate. However, when neutral gas recycling is included, the perfect absorption condition on the plate is relaxed and the effect of the neutral gas evolving from the wall is considered. This will be discussed later in this paper.

It should be emphasized that the boundary at $x = L$ is placed on the plasma side of the sheath edge. The simulation does not enter the sheath itself. However, the requirement of equal ion and electron fluxes to the wall determines the wall potential, Φ_w. The potential drop across the sheath is then given by $(\Phi_1 - \Phi_w)$, where Φ_1 is the potential at $x = L$.

3 Numerical Algorithm

The solution of the Vlasov equation, Eq. (1), for the ion density, n_i, is coupled with Eqs. (2) and (3) in an iterative scheme for the electrostatic potential, $\Phi(x)$. The steps involved in a computational cycle are summarized as follows:

1. Introduce an initial guess for the potential profile.

2. Starting with the first source, particles are launched with randomly chosen velocities according to Eq. (5). For each particle, the time it spends in crossing each cell on the computational grid is computed. This procedure is repeated till all the sources are considered.

3. The density in every cell is calculated from Eq. (8).

4. Quasi-neutrality along the magnetic field line is used to get a *new* potential at every mesh point

$$\Phi_j^{new} = \frac{KT_e}{q} \ln(n_j/n_{eo}). \tag{9}$$

5. Convergence is reached whenever

$$|\Phi_j^{new} - \Phi_j^{old}| < \varepsilon \quad \ldots \; for\; all\; j, \tag{10}$$

where ε is a convergence criterion parameter.

6. Whenever the above criterion is not satisfied, the potential is updated and the ion dynamics are re-computed in the *new* potential starting from step (2).

4 Effect of Neutral Gas Recycling

Ions reaching the target plate get neutralized and a neutral gas evolves from the wall into the edge region. We assume that a fraction δ of this neutral gas is ionized in the edge region producing cold ions. These cold ions are accelerated along the field lines into the target plate. The remaining fraction, $1-\delta$, of the neutral gas is pumped away from the system. The cold electrons produced in the ionization process will thermalize with the Maxwellian electron background. We assume that electron heat conduction along the field line is rapid enough to keep the electron temperature uniform along **B**.

The cold ions produced in the edge region increase the ion density because of their finite transit time to the plate. Quasi-neutrality forces the electron density to increase also, and the potential drop is reduced as implied by the Boltzmann relation.

Throughout our treatment of the effect of neutral gas recycling, the following assumptions are made:

1. The cold plasma density, and consequently the neutral density, is low enough to keep the potential profile monotonically decreasing towards the plate. In future work we will relax this assumption.

2. Only ionization by electron impact is considered. Charge exchange effects are not included at this time.

3. Constant ionization mean free path, λ.

4. The neutral gas transport is described by a simple model for the spatial variation of the neutral gas density of the form

$$n_o = N_o \exp[-(L - x)/\lambda] , \tag{11}$$

where N_o is a normalization constant. The actual neutral density profile depends on the three dimensional geometry of the discharge and divertor chambers, the plasma density and flow velocity, and the details of the vacuum pumping system. Such a complete description of neutral gas transport is beyond the purpose of this work. In fact, the code is not restricted to the model represented by Eq. (11). Any mathematically or numerically calculated neutral gas density profile will work as well.

The cold ions are represented by non-uniformly distributed ion sources

along the computational grid. The cold ion source in the jth cell is given by

$$S_j^{cold} \;=\; n_j\, n_{oj} \;<\sigma\, v>_e \;\Delta x_j\;, \tag{12}$$

where n_j and n_{oj} are the electron and neutral gas densities in the jth cell, respectively. $<\sigma\, v>_e$ is the reaction rate for ionization by electron impact. A neutral gas balance at the plate requires

$$\int_0^L S_j^{cold}\, R(x)\, dx \;\;=\;\; \delta\, \Gamma_w\, R(L)\;, \tag{13}$$

where Γ_w is the total (cold + hot) ion flux to the plate. This is related to the input hot ion flux at $x = 0$, Γ_{in}, by $\Gamma_w \;=\; \Gamma_{in}\,/\,R(L)(1-\delta)$. Here $R(x)$ is the ratio of the field line strength at $x = 0$ to that at point x. Inserting Eqs. (11) and (12) into Eq. (13), the cold ion source in the jth cell is given by

$$S_j^{cold} \;=\; \frac{\delta\, R(L)\, \Gamma_w\, n_j\, \Delta x_j}{I}\;\exp[\,-(1-x/L)\,], \tag{14}$$

where

$$I \;=\; \int_0^L n_j\, R(x_j) \exp[\,-(1-x_j/L)\,]\, dx_j. \tag{15}$$

Once the cold ion source has been determined, particles are launched from every cold source on the computational grid with velocities corresponding to the neutral gas temperature T_i^c and according to the probability formula given by Eq. (5). The same procedure described in Sec. 3 is then followed to calculate the cold ion density in each cell. The cold and hot ion densities are added in every cell and the electrostatic potential is computed from quasi-neutrality.

5 Modeling Considerations

We have used the code described above to simulate plasma flow in the edge region of a stellarator. It is well known that the stellarator family of toroidal confinement systems possesses a natural divertor [9]. This divertor is characterized by a magnetic separatrix, which isolates the confinement region of closed nested toroidal flux surfaces from the surrounding divertor region and the walls of the device. Plasma diffusing out of the main confinement region enters the scrape-off zone and flows along the diverted field lines into the divertor chamber, where it strikes the target plate.

From magnetic field line calculations, a large variation of $|\mathbf{B}|$ along the trajectory of a particle has been computed [10]. This could lead to significant potential variation along the open field line. Calculation of this potential is important for divertor calculations. Figure 2 shows the variation of the magnetic field strength along one field line in ATF-1. The region between the last peak in $|\mathbf{B}|$ and the target plate represents the *fish tail* of the stellarator divertor, which is the region simulated in this work. We assume a parabolic magnetic field profile with $B_o/B(L) = 3$. It should be noted that it is the magnetic field mirror ratio that enters into the calculations and not the absolute value of the magnetic field line strength. Particles streaming out of the main plasma along the diverted field lines into the fish tail region are modeled by a single particle flux source at $x = 0$. As illustrated in Fig. 1, the region $0 \leq x \leq L$ is sourceless if neutral gas recycling at the

neutralizer plate is neglected. Plasma is assumed to be maintained by a hot particle source at $x = 0$. In a real experiment, the input particle flux to the edge region is not a constant but rather determined by the confinement time, and fueling. With neutral gas recycling included, sources with different strength are distributed along the computational region to model the cold ions produced by the ionization of the neutral gas, as described in Sec. 4.

6 Results and Discussion

The first case we simulated was the plasma flow in the fish tail region, neglecting the recycling of the neutral gas at the neutralizer plate. Figure 3 shows the normalized potential profile, $\psi(x) = -e\Phi(x)/KT_e$, along the magnetic field line for three different mirror ratios at the sheath edge. For $R(L) = 1$, the simulation corresponds to the case of a plasma flowing in a uniform magnetic field. The potential at the sheath edge, $\psi_1 = \psi(x = L) = 0.4$, is in good agreement with the analytical results obtained by Emmert *et al.* [8]. As R increases above unity, the influence of the acceleration term due to the magnetic field gradient becomes obvious. The faster motion of the ions results in shorter transit times and hence lower ion density. For quasi-neutrality to be maintained, the electrostatic potential should increase accordingly. Figure 4 shows the variation of the potential at the sheath edge, ψ_1, and that at the wall, ψ_w, with the edge mirror ratio, $R(L)$, in the range $1 \leq R \leq 10$. As R increases, the ion density decreases, as explained above, and consequently

both ψ_1 and ψ_w increase. The response of the potential profile to changes in the ratio of the ion to electron temperature, τ, is shown in Fig. 5. For $\tau > 1$, ions are more energetic and hence there is less need for a large presheath potential drop to accelerate them to enter the sheath with the necessary speed to satisfy the generalized Bohm criterion.

The above results neglect neutral gas recycling. We now include the effect of recycling at the neutralizer plate as discussed in Sec. 4. The potential profiles shown in Fig. 6 are obtained with different amounts of recycling, δ. These profiles are the result of two competing effects. The first is the cold ion source which increases exponentially towards the plate, Fig. 7, and the second is the increased acceleration due to the gradient of the magnetic field, which tends to deplete the ion density as we approach the plate. Therefore, as the amount of the neutral gas recycled in the edge region increases, the potential profile flattens out and the drop across the sheath increases, as shown in Fig. 8. The cold ion contribution to the total ion density is reflected as an increase in the electrostatic potential to maintain quasi-neutrality. As shown in Fig. 8, both ψ_1 and ψ_w decrease with increasing δ.

The electron energy flow to the wall is the value for a Maxwellian electron distribution where the wall potential is determined from the ambipolarity condition. Secondary electron emission is ignored throughout this work. The ion energy flux, Q_i, is evaluated by computing the kinetic energy carried by each particle and summing over the total number of particles. As shown in Fig. 9, the ion energy flux to the sheath, Q_i^1, decreases with δ. This is a

direct consequence of the reduction in the presheath drop with recycling. In crossing the sheath, ions gain an additional amount of energy equal to the sheath potential drop $\Delta\psi_s = (\psi_w - \psi_1)$. Since the sheath drop, $\Delta\psi_s$, increases with δ as shown in Fig. 8, the ion energy flux to the wall, Q_i^w, increases with recycling. On the other hand, the average energy carried by each particle to the wall , $E_{av} = Q_i^w/\Gamma_1$, is lowered by recycling, as shown in Fig. 10. This can be understood by recalling that the particle flux amplification at the plate implies that each input particle at $x = 0$ has more than one chance to carry the input energy to the plate. Therefore, recycling of the neutral gas is one of the methods that can be used to reduce sputtering of the neutralizer plate by keeping the average energy carried by each particle striking it below its material sputtering threshold.

It should be noted that the results presented here are normalized to the electron temperature. Although it was not considered explicitly in this study, recycling also lowers the electron temperature directly and thereby reduces the magnitude of the presheath and sheath potential drop.

7 Conclusions

We have developed a kinetic transport code to simulate the flow of a magnetized plasma to a neutralizer plate. The code has been applied to the divertor region of a stellarator in which the magnetic field strength falls monotonically from the last mirror point to the plate. The recycling of the neutral

gas refluxing from the plate has also been considered. Results show that the presence of a falling magnetic field strength increases the potential difference between the peak magnetic field point and the sheath edge above that obtained with a uniform field calculation. On the other hand, recycling increases the ion density and hence decreases the presheath potential drop. The particle and energy fluxes to the wall are amplified by the contribution of the cold ions produced from ionizing the recycled neutral gas. Also shown is the effect of recycling in reducing the average energy carried by each particle to the neutralizer plate.

Acknowledgement

This research was supported by Martin Marietta Energy Systems, Inc. The authors acknowledge the helpful discussions with J. Rome and R. Fowler of Oak Ridge National Laboratory.

References

[1] Hinton, F. and Hazeltine R., *Phys. Fluids*, **17** (1974) 2236.

[2] El-Nadi, A., *Phys. Fluids*, **22** (1979) 1570.

[3] Daybelge, U., *Nucl. Fusion*, **21** (1981) 1587.

[4] Gierszewski, P., McKenty, P., McCullen, J., and Morse, R., *Phys. Rev. Lett.*, **49** (1982) 650.

[5] Emmert, G. and Bailey, A., *J. Nucl. Mater.*, **93** & **94** (1980) 238.

[6] Bailey, A. and Emmert, G., *Nucl. Fusion*, **40** (1984) 1439.

[7] Whealton, J., Jaeger, E., and Whitson, C., *J. Comp. Phys.*, **27** (1978) 32.

[8] Emmert, G., Wieland, R., Mense, A., and Davidson, J., *Phys. Fluids*, **34** (1980) 803.

[9] Derr, J. and Shohet, J., *IEEE Trans. on Plasma Phys.*, **PS-9** (1981) 234.

[10] Rome, J., Fowler, R. and Emmert, G., *Divertor Calculations for Stellarators*, Int. Stellarator/Heliotron Workshop, Kyoto, Japan (1986).

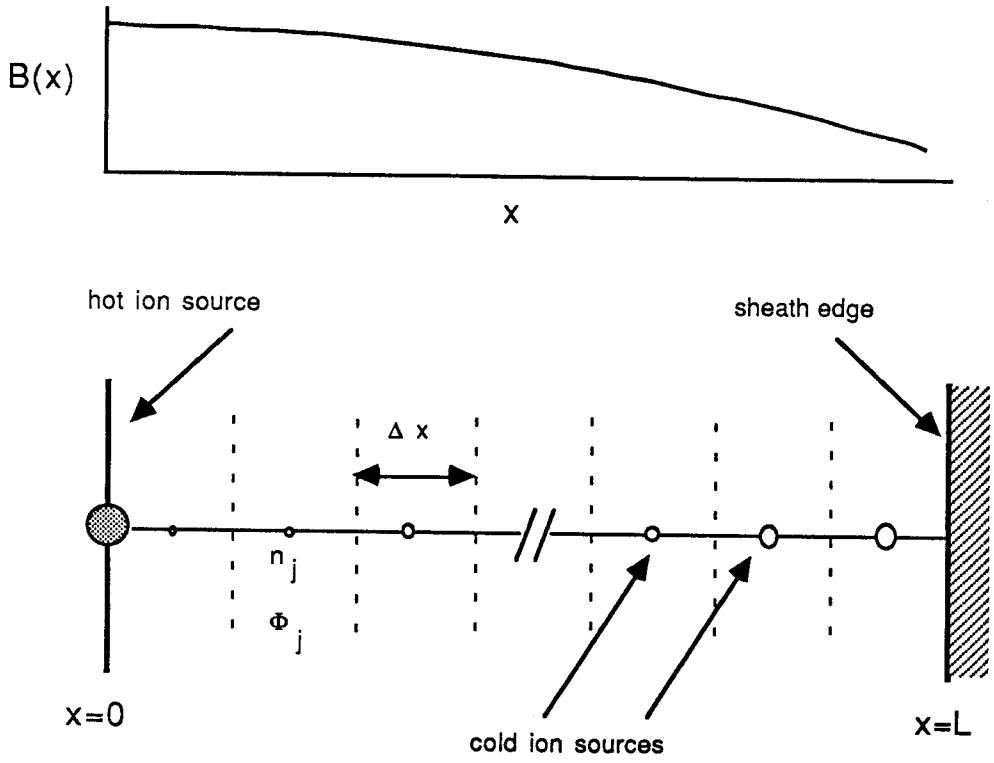

Figure 1: Computational grid.

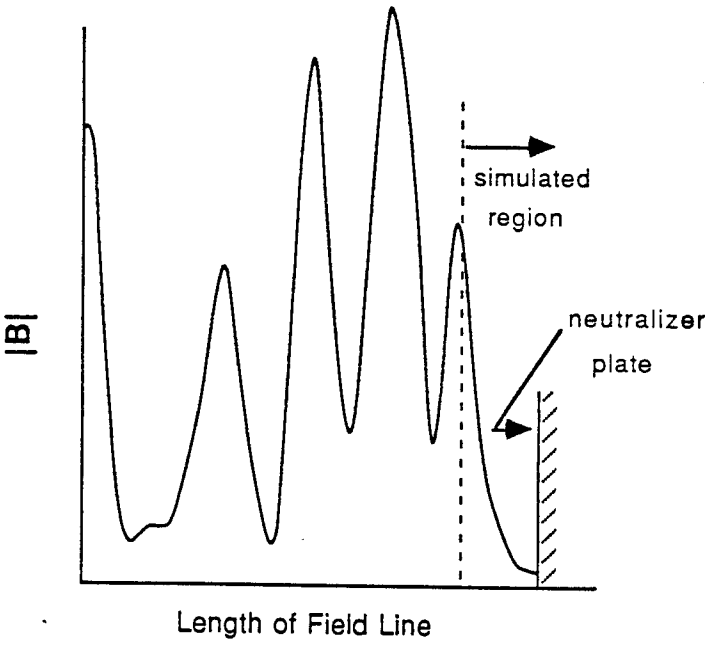

Figure 2: Variation of the strength of one of ATF-1 magnetic field lines.

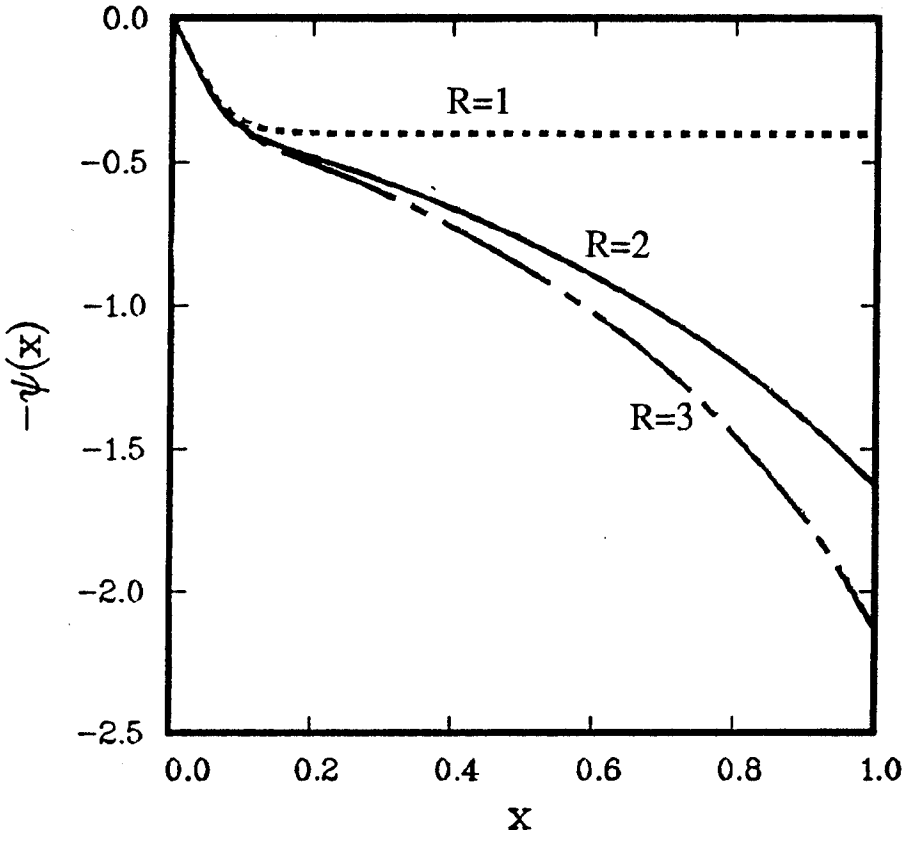

Figure 3: The normalized potential profile $\psi(x)$ for a parabolic magnetic field with different edge mirror ratios, $R(L)$. x is normalized to the distance along a field line, L.

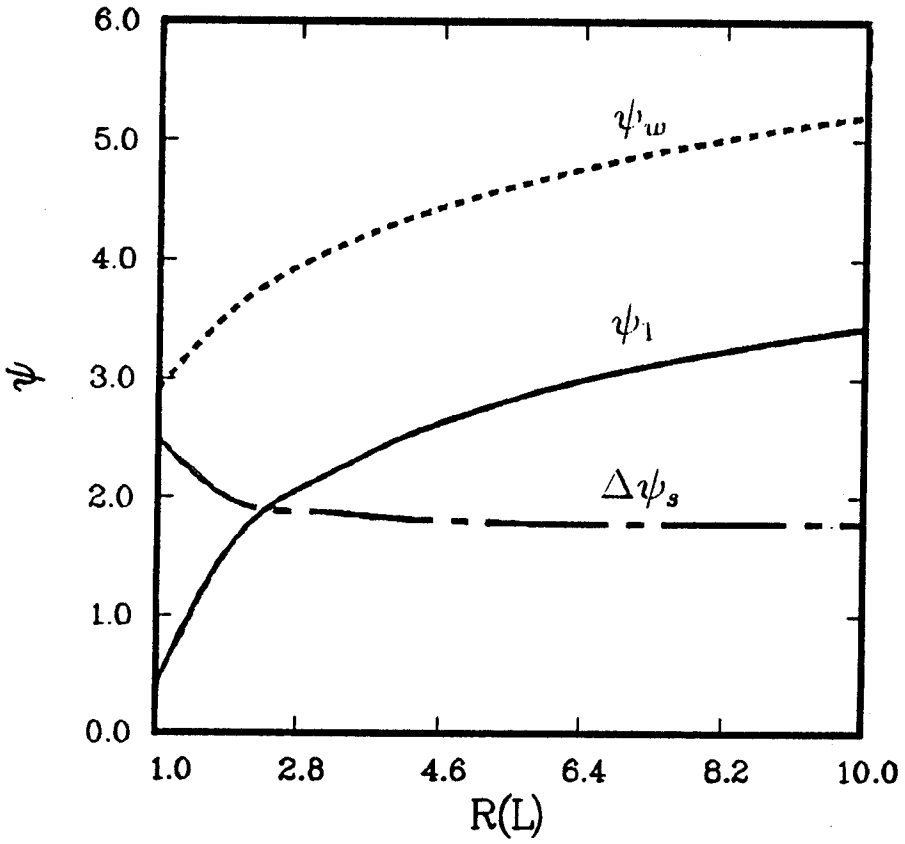

Figure 4: Variation of the normalized potential at the sheath edge, ψ_1, and that at wall, ψ_w with the edge mirror ratio, $R(L)$.

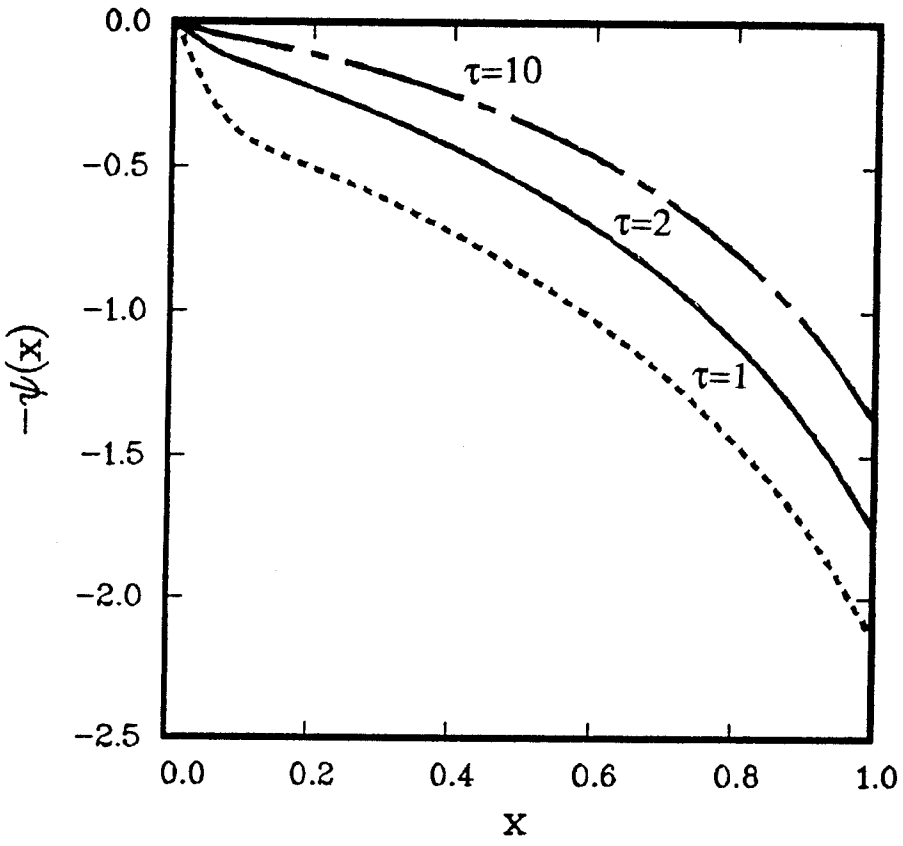

Figure 5: The normalized potential profile $\psi(x)$ for different values of the ion to electron temperature ratio, τ. The edge mirror ratio is 3.

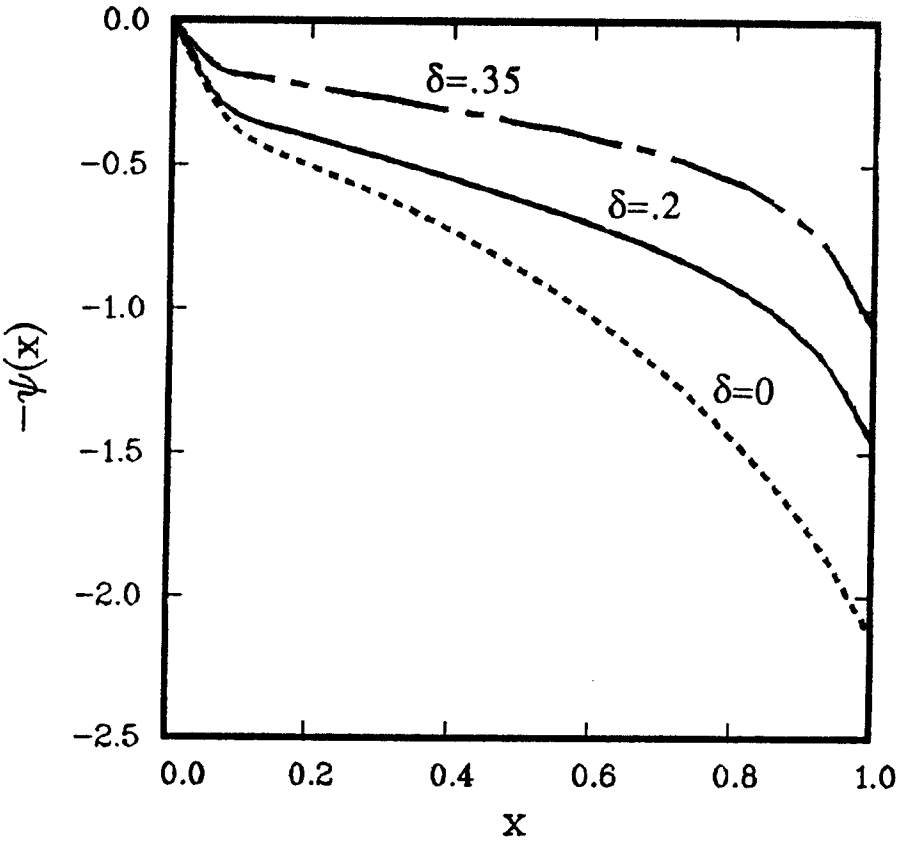

Figure 6: The normalized potential profile $\psi(x)$ for different amounts of recycling, δ. The mean free path for electron impact ionization is $\lambda = 0.1332\,m$.

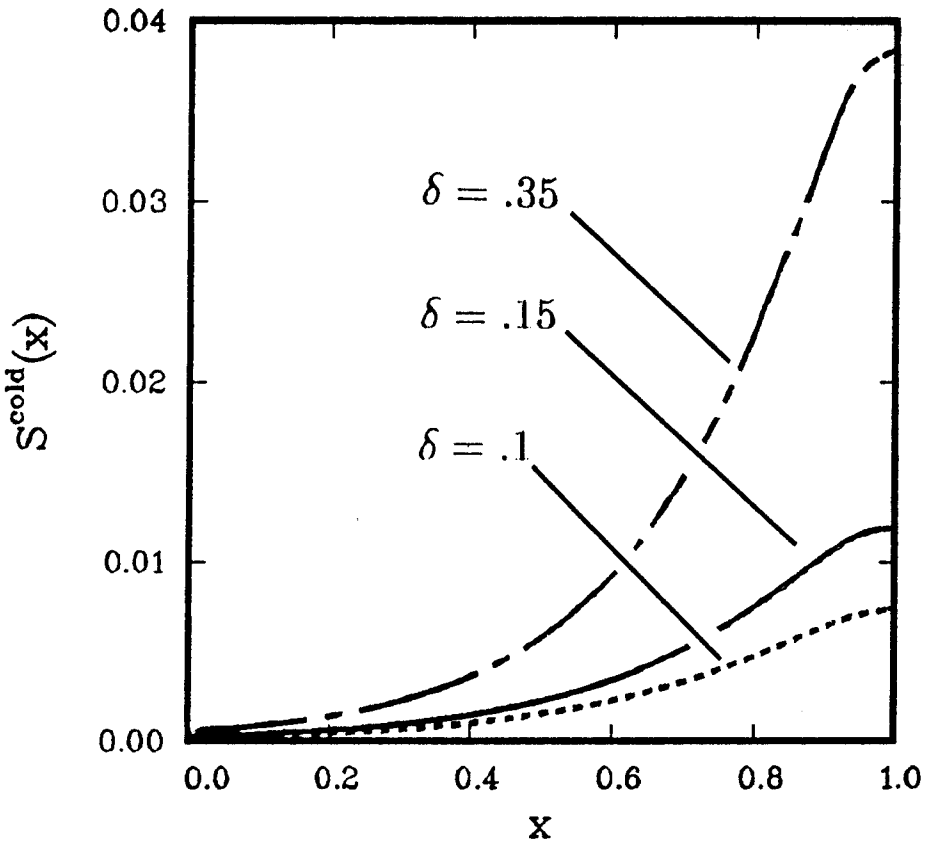

Figure 7: The cold ion source spatial distribution normalized to the hot ion source strength at $x = 0$. The mean free path for electron impact ionization is $\lambda = 0.1332\,m$.

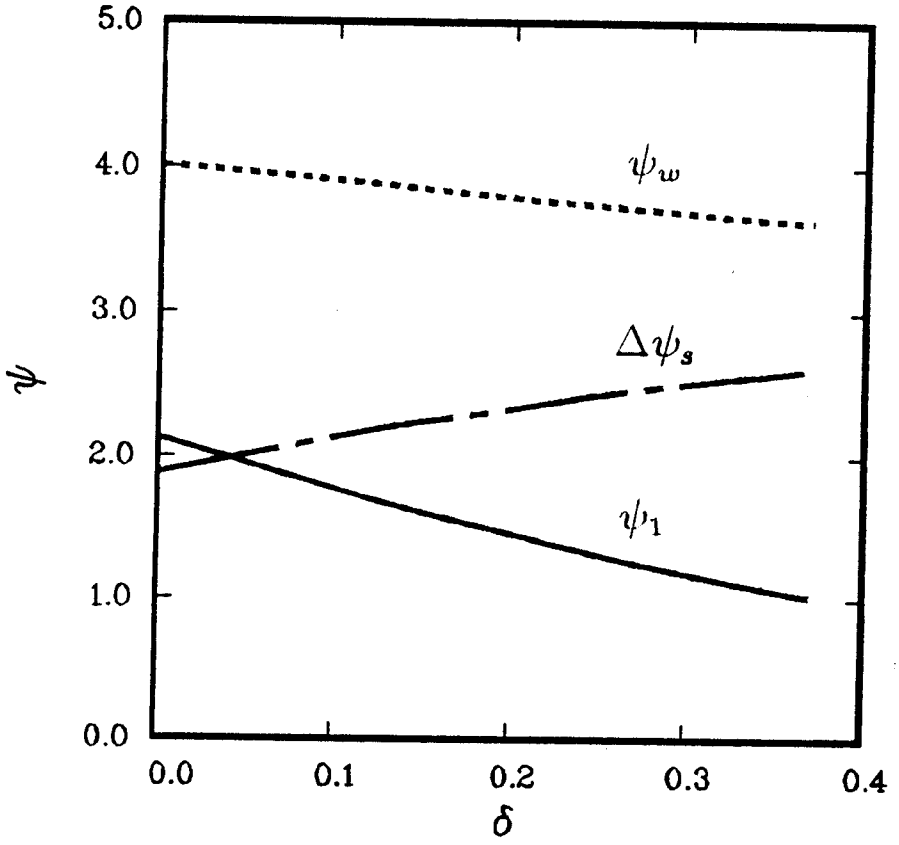

Figure 8: Variation of the normalized potential at the sheath edge, ψ_1, the normalized potential at the wall, ψ_w, the potential drop across the sheath, and $\Delta\psi_s$ with the fraction of the neutral gas recycled, δ.

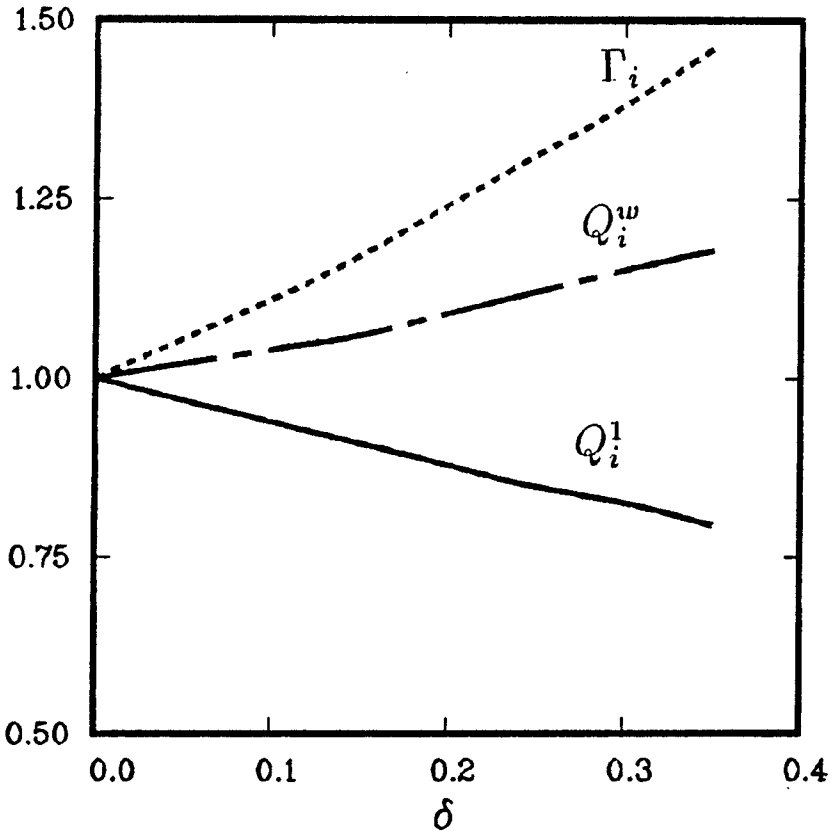

Figure 9: Variation of the ion particle flux to the sheath, Γ_i, the ion energy flux to the sheath, Q_i^1, and the ion energy flux to the wall, Q_i^w, with recycling, normalized to their values with $\delta = 0$.

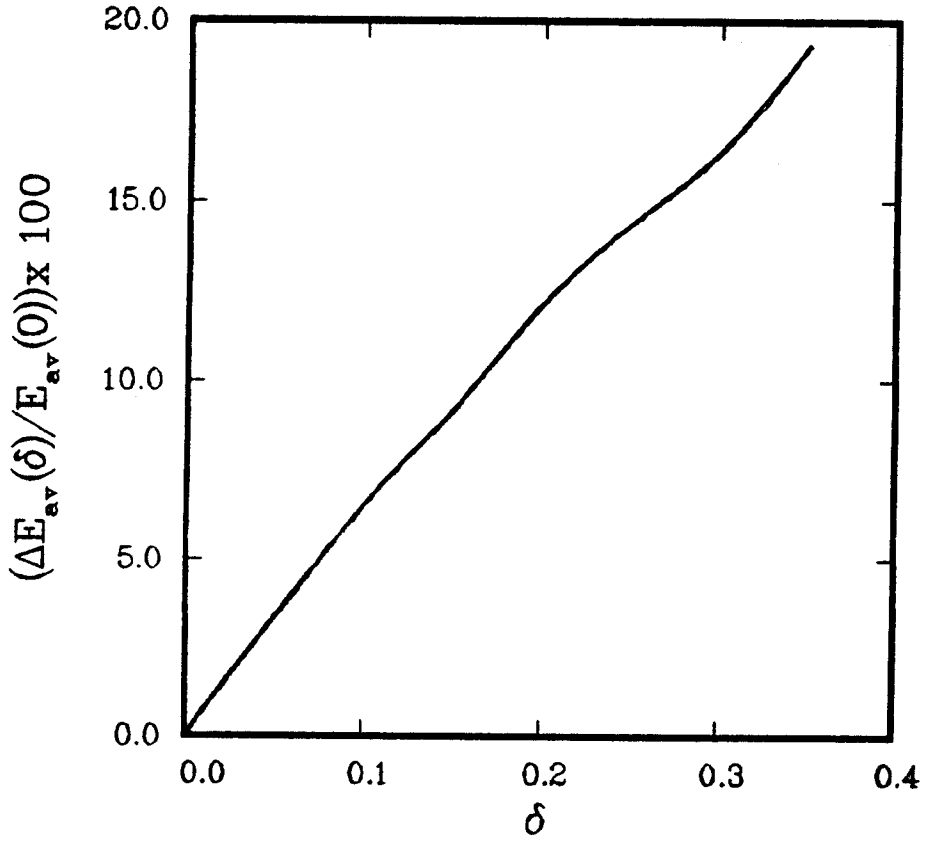

Figure 10: The percentage decrease in the average energy carried by each particle to the wall with recycling.